Quantitative Ultrasound Imaging for the Differentiation between Fresh and Decellularized Mouse Kidneys*

Israa Alnazer, Omar Falou, *Member, IEEE*, Remie Nasr, *Member, IEEE*, Danielle Azar, Eno Hysi, Lauren Wirtzfeld, Elizabeth S.L. Berndl, and Michael C. Kolios, *Member, IEEE*

Abstract— **Decellularization is a technique that permits the removal of cells from intact organs while preserving the extracellular matrix (ECM). It has many applications in various fields such as regenerative medicine and tissue engineering. This study aims to differentiate between fresh and decellularized kidneys using quantitative ultrasound (QUS) parameters. Spectral parameters were extracted from the linear fit of the power spectrum of raw radio frequency data and parametric maps were generated corresponding to the regions of interest, from which four textural parameters were estimated. The results of this study indicated that decellularization affects both spectral and textural parameters. The Mid Band Fit mean and contrast were found to be the best spectral and textural predictors of kidney decellularization, respectively.**

Keywords—Extracellular matrix, quantitative ultrasound, textural analysis.

I. Introduction

End Stage Renal Disease (ESRD) is characterized by the progressive deterioration of renal function. When the kidneys totally fail, either a kidney transplant or dialysis is required to eliminate wastes from the blood. However, the high rate of immune response in addition to the limitation of available organs supports the need for new strategies. Thus, a bioengineering solution, alternative to organ transplantation, has been introduced [1]. It consists of implementing for the patient a decellularized organ, then recellularizing this scaffold with different patient cell sources, which can provide a functional organ with no immune rejection.

Decellularization is a technique that aims to remove cellular and nuclear materials from tissue with chemical, physical, and/or biological agents and preserve only its three-dimensional scaffolds or its extra cellular matrix (ECM) structure which can be used in field of tissue engineering and regenerative medicine [2]–[4]. The ECM consists of proteins and biomolecules synthesized by cells that make up a non-cellular component present within each tissue and organ. It contains an essential physical scaffolding for the cellular constituents and provides crucial biomechanical and biochemical cues that are used in tissue morphogenesis, homeostasis and differentiation [5].

Quantitative Ultrasound (QUS) is a technique that analyses raw ultrasound backscattered signals and provides quantitative information regarding tissue microstructure by extracting parameters from these signals and not from conventional brightness mode (B-mode) ultrasound images. QUS has shown the ability to detect and quantify cell death in response to cancer treatments. It has been investigated for evaluating patient responses to chemotherapy [6]. QUS maps analysis have also been used to provide information about different types of breast tumors [7].

Previous studies have shown that the information regarding scatterer properties of tumors may be extracted from the ultrasound backscattered signals [6], [8]. Some examples of these properties are the effective scatterer diameter, acoustic concentration and attenuation. Moreover, using a linear fit of the power spectrum of ultrasound signals, other parameters may be extracted which have the ability to characterize biological tissues. In addition to the spectral parameters, textural parameters based on the concept of Gray Level Co-occurrence Matrix (GLCM), have been used to improve the categorization efficiency [9], [10].

In this work, we investigate the use of high-frequency quantitative ultrasound techniques for the differentiation between fresh and decellularized kidneys. Both spectral and textural parameters were extracted from mouse kidneys, before and after decellularization. The changes of these parameters after decellularization are presented and discussed.

II. Materials and Methods

A. Decellularization

Decellularization provides the native scaffold of the tissue, the ECM structure. The most commonly utilized methods for

* Research supported by the Canada Foundation for Innovation, the Canada Research Chairs and the Terry Fox New Frontiers Program Project Grant in Ultrasound and MRI for Cancer Therapy (project #1034)

I. Alnazer and R. Nasr are with the Doctoral School of Science and Technology, Lebanese University, Tripoli, Lebanon (e-mails: israa_alnazer@hotmail.com, remie.nasr@gmail.com).

O. Falou is with the Department of Computer Science and Mathematics, Lebanese American University, Byblos, Lebanon; with the Doctoral School of Science and Technology, Lebanese University, Tripoli, Lebanon; and with the Department of Science, American University of Culture and Education, Koura, Lebanon (e-mail: ofalou@gmail.com).

D. Azar is with the Department of Computer Science and Mathematics, Lebanese American University, Byblos, Lebanon (e-mail: danielle.azar@lau.edu.lb).

E. Hysi, L. Wirtzfeld, E. Berndl and M. C. Kolios are with the Institute for Biomedical Engineering, Science and Technology (iBEST), a partnership between Ryerson University and St. Michael's Hospital, Toronto, ON, Canada (e-mails: eno.hysi@ryerson.ca, lauren.wirtzfeld@ryerson.ca, eberndl@ryerson.ca,mkolios@ryerson.ca).

978-1-5386-1311-5/19/$31.00 ©2019 IEEE

removing cells from intact tissues present a combination of physical and chemical treatments [2], [3].

The experimental procedures described in this paper were approved by the Institutional Research Ethics Board. Eight kidneys were decellularized by washing the tissue in sodium dodecyl sulfate (SDS) for 24 hours, then by washing with Triton-X for 24 hours and finally washing and storing in PBS. Thus, the native three-dimensional architecture of the ECM is isolated from tissue cells [11].

B. Data Acquisition

The ultrasound imaging system used was the Vevo 2100 (FUJIFILM VisualSonics, Toronto, ON). Kidneys were imaged using a MS550S linear array transducer, before and after decellularization, using the same machine settings. Data was acquired in 3D-RF mode across the entire kidney, with a step size of 76 μm resulting in ~130 imaging planes per kidney.

C. Data Analysis

For each frame, Regions of Interest (ROIs) corresponding to the medulla were outlined on the reconstructed B-mode image as shown in Fig. 1. Data was processed over a bandwidth of 24-41 MHz corresponding to the –6-dB bandwidth of the transducer [12].

Within each analysis window, power spectrum was calculated for each scan line, corrected using the spectral difference method to avoid the frequency-dependent attenuation of intervening tissues [13], and normalized using the reference phantom technique to be independent of system transfer function and propagation medium attenuation as described in [12]. Then, the backscattered coefficient (BSC) was estimated. Spectral parameters, including Spectral Slope (SS), related to the effective scatterer size and attenuation, the 0-MHz Intercept (SI), related to the effective scatterer size and acoustic concentration, and Mid Band Fit (MBF), related to the effective scatterer size, the acoustic concentration, and the attenuation [14], [15], were extracted from the linear fit of the averaged BSC, which reflects the corrected and normalized power spectrum of the raw radiofrequency data.

Moreover, QUS parametric maps were generated within an ROI by converting estimates of spectral parameters to color coded pixels [16]. Each ROI was segmented using a sliding window approach with 80% overlap between adjacent windows. Each window had dimensions of 0.5 mm by 0.4 mm, the size of the window was selected to cover 10 wavelengths as depth and 16 scan lines as width. Textural features, including contrast (CON), energy (ENE), homogeneity (HOM) and correlation (CORR) were extracted from the GLCM based on Eqs. 1-4. Given an element $\rho(i,j)$ in a $N_g * N_g$ GLCM, where N_g is the number of gray levels, the textural features were defined as follows:

$$CON = \sum_{i-j=0}^{Ng-1} (i-j)^2 \sum_{i=1}^{Ng}\sum_{j=1}^{Ng} \rho(i,j) \quad (1)$$

$$ENE = \sum_{i=1}^{Ng}\sum_{j=1}^{Ng} \rho(i,j)^2 \quad (2)$$

$$HOM = \sum_{i=1}^{Ng}\sum_{j=1}^{Ng} \frac{\rho(i,j)}{1+|i-j|} \quad (3)$$

$$CORR = \frac{\sum_{i=1}^{Ng}\sum_{j=1}^{Ng}(i-\mu_i)(j-\mu_j)\rho(i,j)}{\sigma_i \sigma_j} \quad (4)$$

where μ_i, σ_i are the mean and standard deviation of the i^{th} row of the GLCM and μ_j, σ_j are the mean and standard deviation of the j^{th} column of the GLCM [17].

For each parametric QUS map, sixteen symmetric GLCMs were constructed, according to four directions (0°, 45°, 90º and 135º) and four pixel-to-pixel distances (1 pixel, 2 pixels, 3 pixels, 4 pixels). Contrast, correlation, energy and homogeneity, for each of the 16 GLCMs were calculated and averaged to obtain a mean rotation-invariant textural value, which resulted in 12 textural features (four textural features for each spectral parametric QUS map) [7]. These parameters describe how the spectral parameters vary within the ROIs and quantify their relationship; the contrast feature measures the difference between the lowest and the highest intensities in a set of pixels, the energy measures the frequency of occurrence of pixel pairs, the homogeneity represents a measure of the incidence of pixel pairs of different intensities and the correlation measures the pixel pairs correlation. Textural parameters were introduced in hope to improve the differentiation between fresh and decellularized kidneys.

Finally, the Kruskal–Wallis statistical test was used to establish the statistical significance of each parameter, where p-value < 0.05 is considered significant.

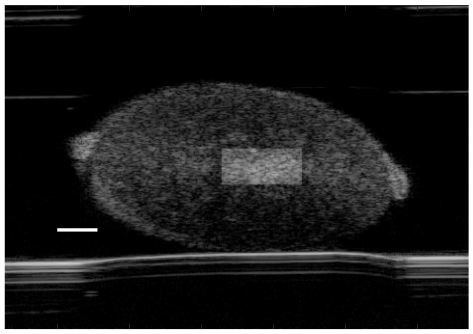

Figure 1. Reconstructed B-mode image of one frame of a kidney. The squares indicate the chosen medulla ROI. The scale bar represents 1 mm.

III. Results and Discussion

A. Spectral parameters

The mean values and the corresponding standard deviations of the spectral parameters for all kidneys, before and after decellularization, for the medulla region are shown in Table I. Both 0-MHz intercept and Mid Band Fit estimated

from kidneys decreased after decellularization contrary to the spectral slope which did not vary on average.

TABLE I. MEAN AND STANDARD DEVIATION OF SPECTRAL PARAMETERS FOR THE MEDULLA REGION

	Cellularized			Decellularized		
	SI (dB)	***SS (dB/MHz)***	***MBF (dB)***	***SI (dB)***	***SS (dB/MHz)***	***MBF (dB)***
Kidney 1	-16.6	0.02	-15.8	-30.7	0.06	-28.6
Kidney 2	-18.4	-0.10	-21.9	-36.0	0.20	-29.3
Kidney 3	-23.0	0.51	-6.21	-38.4	0.22	-31.0
Kidney 4	-19.1	0.17	-13.4	-32.5	0.01	-32.1
Kidney 5	-23.7	0.53	-6.46	-31.1	0.13	-26.8
Kidney 6	-19.6	0.49	-3.61	-41.9	0.30	-32.0
Kidney 7	-26.0	0.14	-21.2	-36.4	0.28	-27.2
Kidney 8	-16.0	-0.16	-21.3	-40.0	0.38	-27.5
Average ± SD	-20.3 ±5.28	0.20 ±0.30	-13.7 ±8.10	-35.9 ±6.29	0.20 ±0.18	-29.3 ±3.07

B. *QUS maps generation*

Parametric maps of SI, SS and MBF were generated using the sliding window analysis by converting spectral parameters values to colored pixels assigned to the appropriate window within the ROI. QUS maps show the variation of these parameters within the corresponding ROI, which gives opportunities to extract additional parameters. Fig. 2 shows QUS images for SI, SS and MBF parameters, corresponding to the medulla region of fresh and decellularized kidneys.

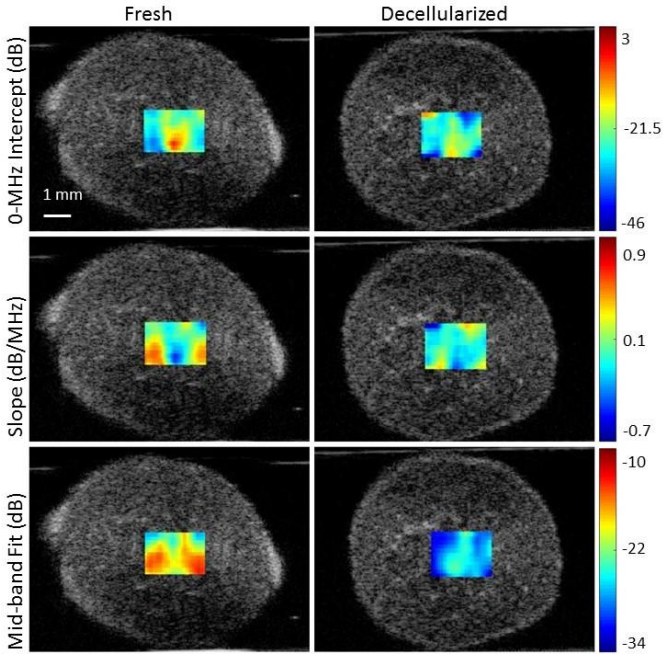

Figure 2. Representative spectral parametric maps from fresh and decellularized kidneys for the medulla region. The scale bar represents 1 mm.

C. *Textural parameters*

The mean value of contrast corresponding to SI, SS and MBF maps increased after decellularization as shown in Fig. 3, contrary to the mean value of correlation and homogeneity of spectral maps which decreased as shown in Figs. 4 and 5. The energy of spectral parameters remained invariant after decellularization. Fig. 6 shows the distribution of fresh and decellularized kidneys corresponding to the MBF mean and MBF contrast parameters, which were found to be the best spectral and textural predictors of kidney decellularization, respectively.

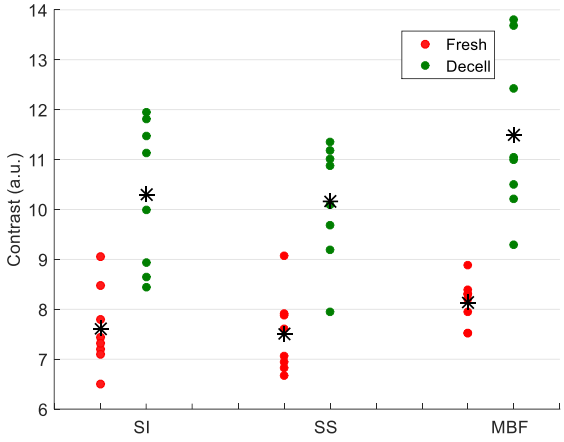

Figure 3. Variation of contrast feature of SI, SS and MBF maps between fresh and decellularized kidneys.

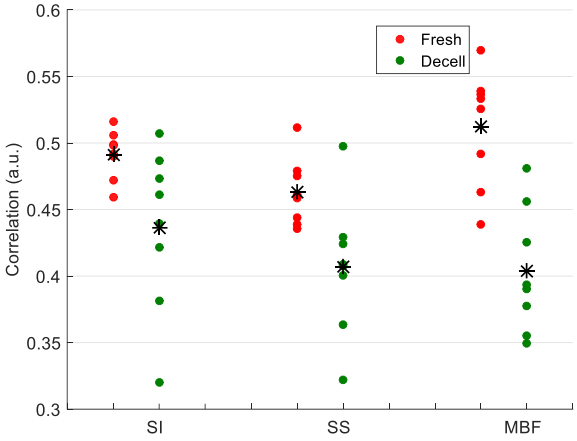

Figure 4. Variation of correlation feature of SI, SS and MBF maps between fresh and decellularized kidneys.

D. *Statistical test*

All the parameters resulted in a *p*-value lower than 0.05 except for the slope (SS) mean, slope (SS) energy, intercept (SI) energy and Mid Band Fit (MBF) energy. Parameters which resulted in a *p*-value greater than 0.05 remained invariant between fresh and decellularized kidneys.

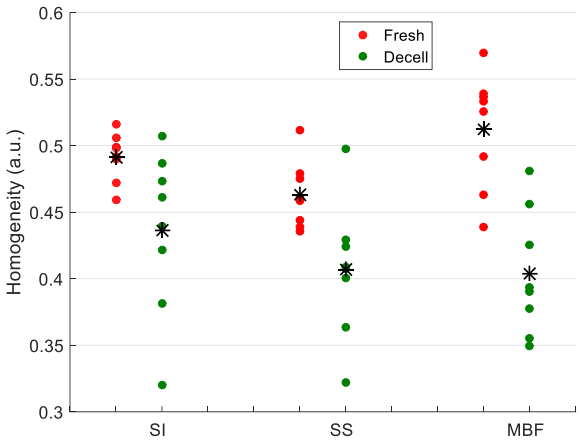

Figure 5. Variation of homogeneity feature of SI, SS and MBF maps between fresh and decellularized kidneys.

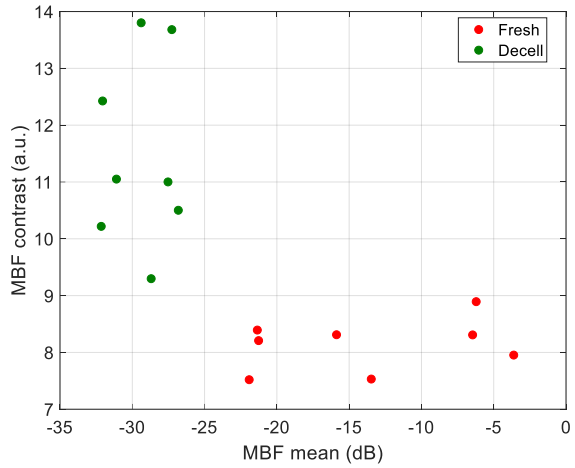

Figure 6. Distribution of fresh and decellularized kidneys corresponding to MBF mean and MBF contrast parameters.

IV. Conclusion and Future Work

The potential of using spectral and textural quantitative ultrasound parameters to non-invasively differentiate between kidneys, before and after decellularization was investigated. The results of this work demonstrated that QUS parameters, particularity the MBF mean and contrast, were able to differentiate between fresh and decellularized kidneys. Future work includes investigating the potential use of quantitative ultrasound imaging to monitor *in vivo* tissue recellularization or regeneration.

Acknowledgments

The authors would like to thank Dr. Gregory J. Czarnota and Dr. Hadi Tadayyon from the Sunnybrook Health Sciences Centre for their helpful advices on various technical issues.

References

[1] A. C. Destefani, G. M. Sirtoli, and B. V. Nogueira, "Advances in the Knowledge about Kidney Decellularization and Repopulation," *Front. Bioeng. Biotechnol.*, vol. 5, no. June, 2017.

[2] L. A. Wirtzfeld, E. S. L. Berndl, and M. C. Kolios, "Ultrasonic Characterization of Extra-Cellular Matrix in Decellularized Murine Kidney and Liver," pp. 3–6, 2015.

[3] R. Nasr, O. Falou, E. Hysi, L. Wirtzfeld, E. S. L. Berndl, and M. C. Kolios, "Differentiation between cellularized and decellularized mouse kidneys using mean scatterer spacing: A preliminary study," *Middle East Conf. Biomed. Eng. MECBME*, vol. 2016-Novem, pp. 120–124, 2016.

[4] R. Nasr *et al.*, "K-nearest neighbor classification for the differentiation between freshly excised and decellularized rat kidneys using envelope statistics," in *Middle East Conference on Biomedical Engineering, MECBME*, 2018.

[5] C. Science and S. Francisco, "The extracellular matrix at a glance," no. December 2010, 2014.

[6] A. Sadeghi-Naini *et al.*, "Quantitative ultrasound evaluation of tumor cell death response in locally advanced breast cancer patients receiving chemotherapy," *Clin. Cancer Res.*, vol. 19, no. 8, pp. 2163–2174, 2013.

[7] H. Tadayyon, A. Sadeghi-Naini, and G. J. Czarnota, "Noninvasive characterization of locally advanced breast cancer using textural analysis of quantitative ultrasound parametric images," *Transl. Oncol.*, vol. 7, no. 6, pp. 759–767, 2014.

[8] H. Tadayyon, A. Sadeghi-naini, L. Wirtzfeld, and F. C. Wright, "Quantitative ultrasound characterization of locally advanced breast cancer by estimation of its scatterer properties."

[9] A. Sadeghi-Naini *et al.*, "Quantitative ultrasound spectral and textural biomarkers of tumor cell death response in breast cancer patients undergoing chemotherapy," in *38th International Symposium on Ultrasonic Imaging and Tissue Characterization (UITC)*, 2013.

[10] A. Sadeghi-Naini *et al.*, "Early prediction of therapy responses and outcomes in breast cancer patients using quantitative ultrasound spectral texture," *Oncotarget*, vol. 5, no. 11, pp. 3497–3511, 2014.

[11] J. Xu, K. Li, R. Smith, J. Waterton, and P. Zhao, "A comparative assessment of preclinical chemotherapeutic response of tumors using quantitative non-Gaussian diffusion MRI," *Magn. Reson.*, 2017.

[12] L. X. Yao, J. A. Zagzebski, and E. L. Madsen, "Backscatter Coefficient Measurements Using a Reference Phantom to Extract Depth-Dependent Instrumentation Factors," *Ultrason. Imaging*, 1990.

[13] L. A. Wirtzfeld *et al.*, "Techniques and evaluation from a cross-platform imaging comparison of quantitative ultrasound parameters in an in vivo rodent fibroadenoma model," *IEEE Trans. Ultrason. Ferroelectr. Freq. Control*, vol. 60, no. 7, pp. 1386–1400, 2013.

[14] F. L. Lizzi, M. Astor, T. Liu, C. Deng, D. J. Coleman, and R. H. Silverman, "Ultrasonic spectrum analysis for tissue assays and therapy evaluation," *Int. J. Imaging Syst. Technol.*, 1997.

[15] F. L. Lizzi *et al.*, "Comparison of theoretical scattering results and ultrasonic data from clinical liver examinations," *Ultrasound Med. Biol.*, 1988.

[16] M. L. Oelze, W. D. O. Brien, J. P. Blue, and J. F. Zachary, "Differentiation and Characterization of Rat Mammary Fibroadenomas and 4T1 Mouse Carcinomas Using Quantitative Ultrasound Imaging," vol. 23, no. 6, pp. 764–771, 2004.

[17] R. M. Haralick, K. Shanmugam, and I. Dinstein, "Textural Features for Image Classification," *IEEE Trans. Syst. Man. Cybern.*, vol. SMC-3, no. 6, pp. 610 – 621, 1973.